
Immunocto: a massive immune cell database auto-generated for histopathology

Mikaël Simard

Medical Physics, UCL, London, UK
m.simard@ucl.ac.uk

Zhuoyan Shen

Medical Physics, UCL, London, UK

Maria A. Hawkins

Medical Physics, UCL, London, UK
Radiotherapy, UCLH, London, UK

Charles-Antoine Collins-Fekete

Medical Physics, UCL, London, UK

Abstract

With the advent of novel cancer treatment options such as immunotherapy, studying the tumour immune micro-environment is crucial to inform on prognosis and understand response to therapeutic agents. A key approach to characterising the tumour immune micro-environment may be through combining (1) digitised microscopic high-resolution optical images of hematoxylin and eosin (H&E) stained tissue sections obtained in routine histopathology examinations with (2) automated immune cell detection and classification methods. However, current individual immune cell classification models for digital pathology present relatively poor performance. This is mainly due to the limited size of currently available datasets of individual immune cells, a consequence of the time-consuming and difficult problem of manually annotating immune cells on digitised H&E whole slide images. In that context, we introduce Immunocto, a massive, multi-million automatically generated database of 6,848,454 human cells, including 2,282,818 immune cells distributed across 4 subtypes: CD4⁺ T cell lymphocytes, CD8⁺ T cell lymphocytes, B cell lymphocytes, and macrophages. For each cell, we provide a 64×64 pixels² H&E image at $40\times$ magnification, along with a binary mask of the nucleus and a label. To create Immunocto, we combined open-source models and data to automatically generate the majority of contours and labels. The cells are obtained from a matched H&E and immunofluorescence colorectal dataset from the Orion platform, while contours are obtained using the Segment Anything Model. An advantage of Immunocto is that immunofluorescence data largely facilitates cell type recognition and thus requires limited annotations. A classifier trained on H&E images from Immunocto produces an average F_1 score of 0.74 to differentiate the 4 immune cell subtypes and other cells. For the more general task of identifying lymphocytes, the classifier trained on Immunocto strongly outperforms a state of the art cell segmentation and classification model, producing an F_1 score of 0.84 compared to 0.10. Immunocto can be downloaded at: <https://zenodo.org/uploads/11073373>.

1 Introduction

1.1 Overview

Histopathology relates to the observation of abnormal tissue at the microscopic scale. The gold standard methodology for histopathology is the study of fixed tissue sections under a microscope stained with haematoxylin and eosin (H&E). To identify diseases, pattern recognition at various

scales on tissue samples is performed by a pathologist. The advent of digital pathology, where tissue sections are digitised to create gigapixel whole slide images (WSIs), opens the possibility of creating large databases to train models that may aid pathologists in their study of diseases and decision making processes.

In the study of cancer, understanding the role of the tumour immune micro-environment (TIME) is essential [1], as it can advise on prognosis, guide treatment [2, 3], or be examined retrospectively to understand response to therapies. For instance, an exploration of the TIME may reveal biomarkers that could be useful in identifying patient populations that respond well to immunotherapy [1].

Microscopic high-resolution imaging, where immune cell location and function can be identified, is a critical next step to understand the TIME, as it can provide information on cellular proportions, heterogeneity and spatial distribution [1]. However, manual annotation of immune cells by pathologists is time consuming and identifying various immune cell subtypes can be tedious on H&E WSIs [4]. As such, there is growing interest in developing models that can automatically segment and classify immune cells on WSIs [5].

As a first step towards building models that can recognise immune cells in WSIs, we introduce Immunocto, a high-resolution ($40\times$ magnification, pixel size of $0.325\ \mu\text{m}$) massive database of 2,282,818 immune cells distributed across 4 immune cell subtypes (CD4^+ T cells, CD8^+ T cells, B cells, and macrophages). To our knowledge, Immunocto is the largest available dataset of immune cells extracted from H&E WSIs by an order of magnitude (table 1).

The main advantage of the methodology used to create the database is that it requires minimal manual annotations, as it combines the Segment Anything Model (SAM) [6] to extract candidate cells and relies on fully registered immunofluorescence (IF) data from the Orion platform [7] to provide labels for candidate cells.

Table 1: Fully labelled and segmented immune cells datasets (≥ 10000 cells) on H&E WSIs. For cell subtypes, L is lymphocyte, M is macrophage, N is neutrophil, P is plasma, and E is eosinophil.

Dataset	Cells	Cancer location	Cell subtypes
MoNuSAC [8]	25,157	Breast, Kidney, Lung, Prostate	L, M, N
PanNuke [9]	32,276	19 sites	L, M, P
NuCLS [10]	47,113	Breast	E, L, M, N, P
Lizard [4]	138,307	19 sites	E, L, N, P
Immunocto	2,282,818	Colon	L (CD4^+ T cell, CD8^+ T cell, B cell), M

1.2 Existing work

There have been considerable efforts in building labelled datasets for nuclear segmentation and/or classification on H&E WSIs. The MoNuSAC dataset [8] contains over 25,000 manually labelled immune cells. Manual labelling of various type of immune cells, which often present similar morphological features, can be cumbersome, requires extensive pathologist time and does not scale well. The PanNuke database [9] rather relied on active learning, where pre-labelled data is used to train a cell subtype classifier, and the results are manually verified by pathologists. The PanNuke database is obtained after 7 iterations between model training and pathologist verification. Still, manual investigation has a limited inter-observer reproducibility due to the above-mentioned reason, which limits the accuracy of this methodology. Alternatively, the larger NuCLS database [10] was obtained with a crowdsourcing approach combining pathologists and non-pathologists (medical students and graduates), which also needs important human intervention and is still limited in accuracy by human identification on H&E images only. More recently, the Lizard database [4] uses a four-step approach - iterative segmentation and classification, cell boundary refinement, inflammatory nuclei subtyping, and manual class refinement. Each step involves important pathologist annotation, and the overall process includes the manual annotation of over 70,000 immune cells.

There are two main limitations of the above datasets which motivated the development of Immunocto. First, **existing datasets involve important human intervention to generate cell labels and/or nuclei masks, which limits the number of labelled immune cells that can be produced.** Second, as the above datasets are obtained using H&E data only, **the accuracy of the underlying labels**

is limited. For instance, the Lizard database [4] has reported limited inter-observer agreement for immune cell identification.

Furthermore, there have only been few investigations into subtyping lymphocytes, which is a difficult and subjective task on H&E images due to morphological similarities between lymphocyte types [11, 12]. For instance, lymphocytes can be, amongst others, classified as CD8⁺ killer (cytotoxic) T cells, CD4⁺ helper T cells, or B cells. Each type has a different function, and capturing the spatial distribution of lymphocytes is an important part of understanding the TIME [1]. As an example, stratification of colorectal cancer patients has been correlated with deep infiltration of CD8⁺ T cells [13], and the CD4⁺/CD8⁺ ratio of tumour-infiltrating lymphocytes has high prognostic value in triple-negative breast cancer [14].

1.3 Key Innovations

Immunocto presents two key innovations. First, we use the Segment Anything Model (SAM) to generate high-quality object masks at the cellular level. This includes, but is not limited to, nuclear structures, epithelial and endothelial cells, muscular and fat cells, apoptotic bodies, blood cells, immune cells, and a variety of gaps and holes in the tissue.

The second innovation lies in the usage of IF as a tool to facilitate cell labelling. IF is a technique that uses antibodies conjugated with fluorophores to detect specific proteins on or within cells. When incubated with tissue sections, the fluorescent antibodies will selectively bind to specific antigens. Irradiating the sample using a laser with a wavelength that matches a fluorophore’s absorption spectrum will create an IF image of the tissue specimen, revealing locations on the tissue where a particular antigen is expressed. For instance, the presence of CD4⁺ lymphocytes can be revealed with CD4 antibodies. In that context, IF can be used to characterise various cell types based on their unique surface markers, including CD4⁺, CD8⁺ T cells, or B cells, the latter with CD20 antibodies. When an IF image is co-localised with an H&E image, an opportunity arises to automatically create a large scale single-cell database, considering the unique object identification originating from the SAM.

In this study, we used the Orion dataset [7], (distributed under the MIT license) which contains H&E images co-localised with 18 IF data channels, to extract cells that are active on IF images associated with immune cells.

2 Creating Immunocto

The overall framework for creating Immunocto is illustrated in figure 1; the 5 steps shown in the figure are detailed in section 2.2. Briefly, SAM is used on a single WSI to detect objects, which are mostly cell nuclei. Using co-localised IF data and a thresholding approach, 20,000 candidate immune cells are automatically extracted from the SAM-derived masks. The cells are manually reviewed by non-pathologists by looking at relevant IF channels. The result is Immunocto V_0 , the first iteration of the database containing 11,321 immune cells and 9048 other cells. This database is used to train a model which predicts an immune cell type using H&E, IF images, and the binary mask from SAM. The model is ran on 40 WSIs with matched H&E and IF data, and a final, highly specific database, Immunocto V_1 , is extracted by only preserving cells with high classification probability (> 95%).

2.1 Raw data source

To create Immunocto, we use 40 colorectal cancer patients with publically available, registered H&E and IF data from the Orion platform proposed by Lin et al. [7]. WSIs are obtained at 40× magnification with a pixel size of 0.325 μm . IF data refers to a set of 18 fluorescence images which are registered to H&E whole slide images and obtained via incubation with various IF markers rather than H&E staining. Briefly, a tissue section is incubated simultaneously with 18 IF markers, each tagging a specific type of cell or structure. For instance, the Hoechst marker identifies nuclei, while the CD20 marker selectively tags B cell lymphocytes. A fluorescence microscopy system using various excitation lasers and tunable filters captures an image for each IF marker, and the pixel-wise intensity of each image is proportional to the concentration of the dye in that pixel. H&E staining and imaging is then performed on the same tissue section.

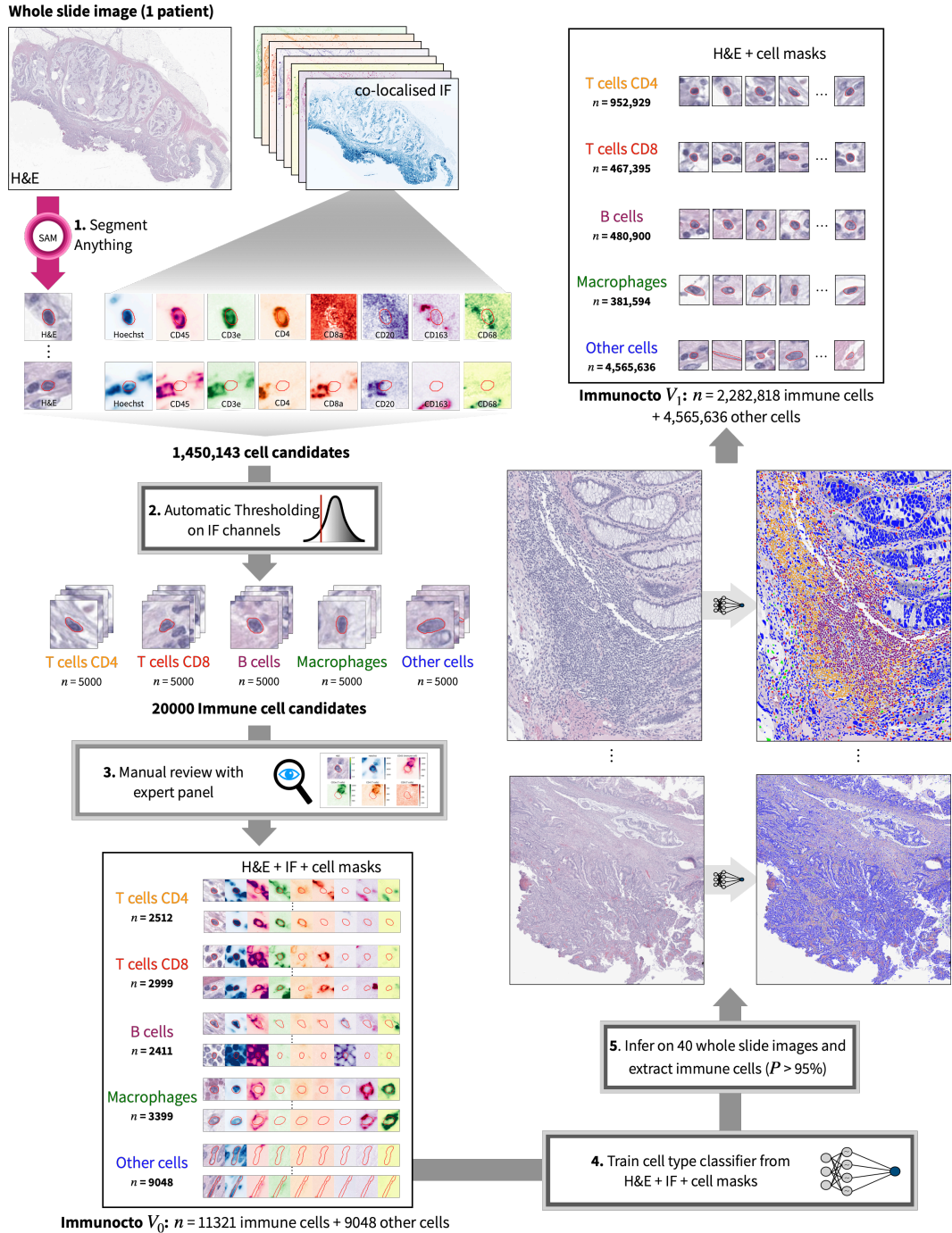


Figure 1: Workflow to create the Immunocito database.

Examples of H&E along with IF data can be seen in figure 1, as well as figure 3 of the supplementary material. With simple thresholding on selected IF channels, one can extract regions of interest associated with specific cell types and generate ground truth labels.

2.2 Database creation steps

Detecting cells with Segment Anything. Cell nuclei in a given WSI can be accurately segmented using SAM [6] (ViT-H architecture) without further fine tuning, provided adequate subsequent

mask filtering. To extract nuclei masks, a WSI is tessellated into non-overlapping tiles of 512×512 pixels². Each tile is resampled to 1024×1024 pixels², and a grid of 64×64 uniformly distributed points across the image is used as a point prompt. Resulting masks are filtered with the following empirically defined criteria: predicted intersection over union (IoU) score of > 0.81 , a stability score > 0.85 , and an area between 42 and 4320 pixels² to cover typical immune cell sizes. Masks with overlapping bounding boxes of IoU larger than 0.1 are discarded via non-maximum suppression using the `batched_nms` operator from PyTorch, with scores interpreted as the original IoU provided by SAM. Resulting masks are arrays of 64×64 pixels². An example of cell detection with SAM over a large region of interest is shown in the first three panels of figure 2.

Generating immune cell candidates via automatic thresholding. Applying SAM on a WSI results, on average, in $> 1,000,000$ detected objects, most of which are cell nuclei. Leveraging IF data, one can extract candidate objects for immune cells using an intensity thresholding scheme detailed in supplementary material section B. For instance, detected objects which present high signal in the Hoechst, CD3e and CD4 IF channels are classified as CD4⁺ T cell lymphocytes. Overall, 25,000 candidate cells are automatically generated - 5000 for each of the four immune cell subtype, and 5000 other, non-immune cells.

Manual reviewing using an expert panel. The automatic thresholding method produces misclassified candidate cells due to imperfections with the IF staining. This includes slight registration errors between IF and H&E channels, non-specific targeting of IF markers and a mismatch between the SAM masks, which contour the nuclei, and the IF signal, typically located on the cytoplasm of cells around the nuclei. Therefore, all candidate cells are manually reviewed by an expert panel (supplementary material section B.2) and re-classified if needed. The presence of the IF channels allows non-pathologists to classify cells, as classification is not based on morphological features of H&E images but mainly on the intensity of selected IF channels. Manual review was performed by three authors of this study (MS, ZS, CACF) using Label Studio v1.10.1 (<https://labelstud.io>). Some cells marked as uncertain by one individual were reviewed by at least another person before assigning a label. The resulting database, Immunocto V_0 , contains 11,321 immune cells (2512 CD4⁺ T cells, 2999 CD8⁺ T cells, 2411 B cells and 3399 macrophages), as well as 9048 other cells.

Training a immune cell classifier from H&E, IF and cell masks. We hypothesise that the above steps - recognising immune cells based on matched IF and H&E data - is a relatively simple task that can be automated with a trained deep neural network. Using the initial dataset Immunocto V_0 , we trained a model that classifies a 12-channel 64×64 pixels² image (which combines H&E, selected IF channels and the binary mask from SAM) into one of five cell types - CD4⁺ T cell, CD8⁺ T cell, B cell, macrophage, and other, non-immune cell. All training details and classification performance metrics are provided in supplementary material section C.

Automatic generation of a massive database of immune cells. The model trained on joint H&E and IF data is applied to the entire cohort of the Orion platform [7], which contains 40 colorectal cancer whole slide images. There are overall 54 million objects detected with SAM on the 40 WSIs; to maximise the quality of automatically generated labels, we only preserve immune cells which have a probability (softmax of logit resulting from the model) above 95%. This results in Immunocto V_1 , the final Immunocto dataset, which contains 2,282,818 immune cells (952,929 CD4⁺ T cells, 467,395 CD8⁺ T cells, 480,900 B cells and 381,594 macrophages). Additionally, Immunocto V_1 includes 4,565,636 (twice the number of immune cells) other, non-immune cells to provide a database that can be used to discriminate generally between immune and non-immune cells. To ensure a wide range of sampled cells, we randomly sampled the 4,565,636 other cells from the subset of objects in all 40 WSIs that were classified as other cell with $> 90\%$ probability.

2.3 The final Immunocto database

The steps from section 2.2 result in Immunocto V_1 , which is the final Immunocto database containing a total of 6,848,454 cells. For each cell, we provide (1) a 64×64 pixels² H&E image at $40 \times$ magnification, (2) a 64×64 pixels² binary mask of the nucleus, and (3) a label. The central point of the bounding box surrounding the cell is located coincides with the center of the images. We provide additional dataset documentation in supplementary material section A.

3 Applications

3.1 Evaluation of H&E classifiers trained on Immunocito on an internal hold-out dataset

To demonstrate the versatility and clinical relevance of the Immunocito dataset, we trained a model that predicts the immune cell subtype (CD4⁺ T cells, CD8⁺ T cells, B cells, macrophages or other, non-immune cell) using solely H&E stained images and cell masks (which can be obtained from SAM, or any other segmentation algorithm).

The approach aims to demonstrate the utility of Immunocito using data accessible in routine clinical practice, where immunofluorescence is not readily available. Such a model could prove invaluable in two key situations: firstly, as a prior assessment of biopsies/resections to guide treatment decisions. Secondly, as tool for analysing the TIME either in low-ressource settings where advanced staining techniques may be inaccessible, or for retrospective studies where only H&E data is available.

To evaluate the performance of the classifier based on H&E data, we set aside an internal hold-out dataset consisting of a single patient from the Orion dataset and used the remaining 39 patients to train the model; training details are reported in supplementary material section D.

We assessed immune cell classification based on H&E images solely using two different approaches. In the first approach, a classifier was trained using patches of 64×64 pixel², which contains information about individual cell morphology. When reporting results, this model is presented as *morph.* (64×64). In the second approach, the classifier was trained with larger patches of 256×256 pixel², enabling it to integrate information concerning the individual cell as well as its interactions with its immediate surrounding environment - this model is presented as *morph. + context* (256×256). Results on the hold-out test dataset are shown in table 2. The table showcases performance metrics including precision (P), recall (R), F_1 score (F_1) for each cell type for classifiers with the two patch sizes. We also reported aggregated scores for other tasks such as identifying T cells (CD4⁺ and CD8⁺) and lymphocytes (T cells and B cells).

Table 2: Prediction metrics (precision P, recall R and F_1 score) on the Orion hold-out patient per cell type. Results are reported for each model - the *morph.* 64×64 captures the cell morphology, while *morph. + context* 256×256 additionally captures the interaction of the cell with its immediate environment. The last two cell types (T cells and lymphocytes) represent aggregated classes.

Cell Type	morph. (64×64)		morph. + context (256×256)	
	P/R	F_1	P/R	F_1
B cells	0.75/0.69	0.72	0.78/0.80	0.79
CD4 ⁺ T cells	0.60/0.62	0.61	0.63/0.66	0.65
CD8 ⁺ T cells	0.54/0.59	0.56	0.57/0.57	0.57
Macrophages	0.61/0.89	0.73	0.65/0.94	0.77
Others	0.99/0.93	0.96	0.99/0.94	0.96
T cells (CD4 & CD8)	0.89/0.95	0.92	0.91/0.94	0.93
Lymph. (T & B cells)	0.92/0.97	0.94	0.94/0.97	0.95

We find that classification of immune cells with the larger context window maximises the F_1 score for all classification tasks shown in table 2. The improvement in F_1 score is most important for immune cell subtyping (notably B cells, CD4⁺ T cells and macrophages), while context only provides limited improvements for general lymphocyte detection.

3.2 Comparison with a state-of-the-art cell detection model

The above classifiers are compared with the state-of-the-art cell detection model HoVer-Net [5] trained on the extensive cell dataset Lizard [4], which was the published database with the highest number of annotated immune cells on H&E datasets prior to this work. HoVer-Net simultaneously performs cell segmentation and classification on H&E images. Since images in the Lizard database have a pixel size of $0.5 \mu\text{m}$ and the hold-out Orion WSI has a pixel size of $0.325 \mu\text{m}$, the hold-out WSI was downsampled to $0.5 \mu\text{m}$ before applying HoVer-Net.

As HoVer-Net was not trained for lymphocyte subtyping, all models are compared on the binary task of identifying if a cell is a lymphocyte or not. For the models trained on Immunocito, a cell is assumed

to be a lymphocyte if it is either a CD4⁺ T cell, CD8⁺ T cell or a B cell. The models were applied on two large regions of interest (ROI) from the hold-out Orion patient. The first region, ROI 1, is a 3849×3850 pixels² patch containing a small number of lymphocytes, while the second, ROI 2, is a 2800×3850 pixels² patch with a high lymphocyte count. Table 3 reports the quantitative performance of the models on the two ROIs, while figure 2 illustrates an overlay of ROI 2 with the segmentation and classification results from the Immunocto models and HoVer-Net. Figure 4 in supplementary material section E.2 illustrates the overlay for ROI 1.

Table 3: Prediction metrics of lymphocyte detection on a region with sparse lymphocytes (ROI 1) and a region with dense lymphocytes (ROI 2) from the Orion hold-out patient.

ROI	# lymph.	# other cells	morph. (64×64)		morph. + context (256×256)		HoVer-Net	
			P/R	F1	P/R	F1	P/R	F1
1	635	10,369	0.43/0.83	0.56	0.45/0.86	0.59	0.53/0.20	0.29
2	4,724	4,566	0.85/0.93	0.89	0.81/0.96	0.88	0.54/0.03	0.06
Total	5,359	14,935	0.77/0.92	0.84	0.75/0.96	0.84	0.54/0.05	0.10

Overall, we find that classifiers trained on Immunocto largely outperforms HoVer-Net for lymphocyte identification. As noted in table 2, context does not provide significant performance enhancements for the general task of classifying lymphocytes. While the HoVer-Net model has generally appreciable precision, its recall is limited. This can be observed in figure 2d, where most of the lymphocytes could not be detected with HoVer-Net. The difference in performance may be attributed to the large discrepancy in the number of training examples for lymphocytes between the Immunocto and Lizard datasets. In addition, the lymphocyte labels provided by Immunocto are based on IF and may be more robust than the manual ones from Lizard, which have limited inter-observer agreement, as noted in figure C.1 of [4].

3.3 Challenges and limitations

Lymphocyte subtyping using co-localised H&E and IF data is a relatively simple computer vision classification task that results in high F_1 scores, between 0.92-0.96 across classes (table 1 of supplementary material). However, when classification is performed solely on H&E images, table 2 shows largely reduced F_1 scores for lymphocyte differentiation. This suggests that subtyping lymphocytes on H&E images only is a difficult task due to their morphological similarities [11, 12]. Therefore, the Immunocto dataset could be used to benchmark more advanced computer vision models for classification.

The main limitation of Immunocto is that it has been trained only on colorectal cancer data, as opposed to most other databases reported in table 1; this may limit the generalisation capabilities of models trained on Immunocto for pan-cancer immune cell detection.

4 Conclusion

Immunocto is the largest available database of segmented immune cells on H&E whole slide images for histopathology. It is automatically generated using matched immunofluorescence data and SAM for object segmentation. It contains 952,929 CD4⁺ T cells, 467,395 CD8⁺ T cells, 480,900 B cells and 381,594 macrophages, as well as 4,565,636 other non-immune cells. The database can be used to train models to study the tumour immune micro-environment on routine H&E whole slide images. We report state of the art performance on immune cell detection and subtyping using simple classifiers trained on Immunocto.

Furthermore, the methodology used to generate Immunocto can be extended to more cell types, given that matched IF data is available. The approach demonstrates the benefits of using matched H&E and IF data to generate robust databases for computational pathology.

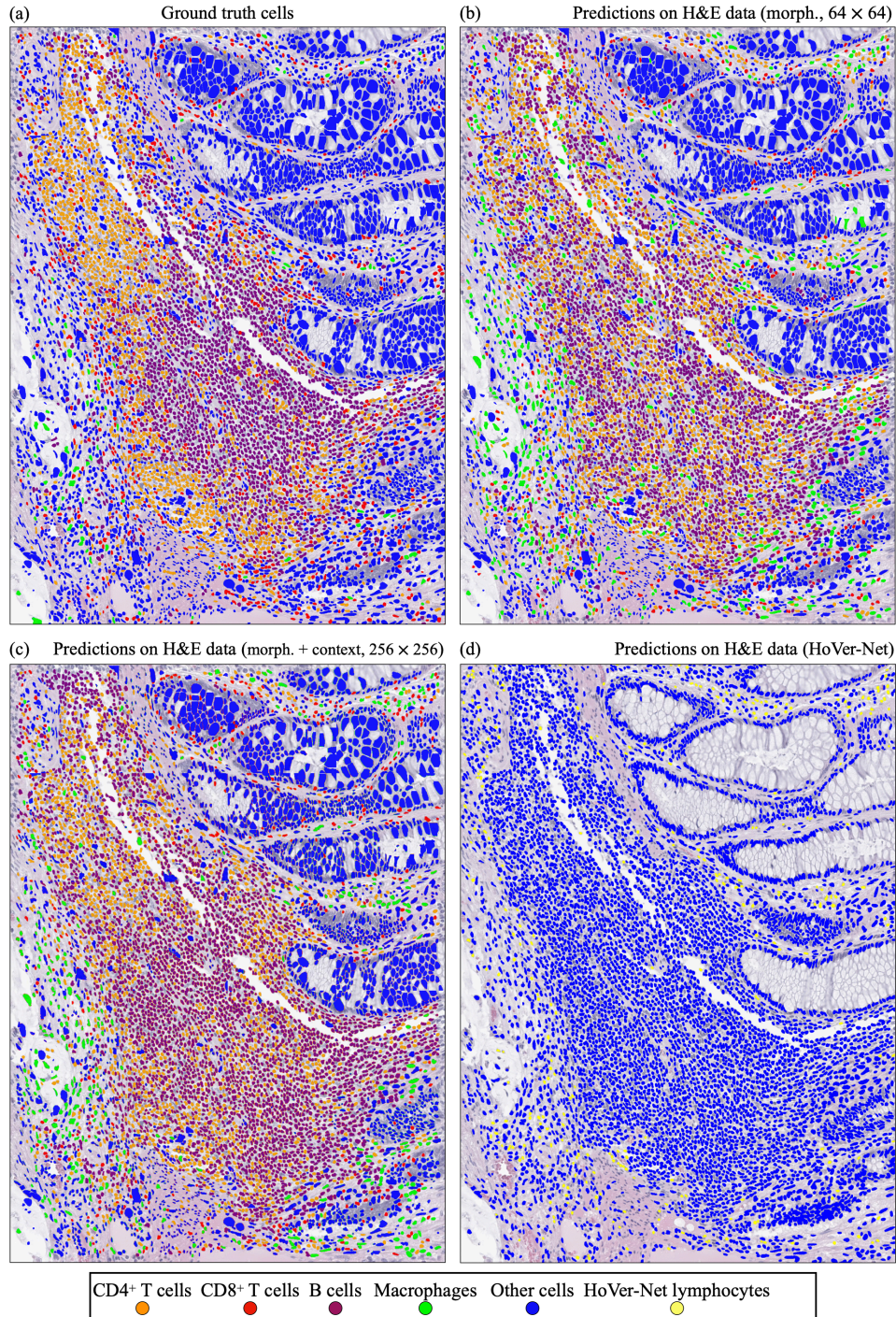


Figure 2: Overlay of a H&E region of interest containing a high lymphocyte count with predicted cell types from various models. (a) shows the ground truth labels from the Immunocito database; (b) and (c) respectively show the predictions from the morph. 64×64 and morph. + context 256×256 models trained on the remaining Immunocito data. (d) shows the predictions using HoVer-Net.

Acknowledgments and Disclosure of Funding

This project is supported by the UKRI Future Leaders Fellowship, No. MR/T040785/1, the Radiation Research Unit at the Cancer Research UK City of London Centre Award C7893/A28990, as well

as the UKRI AI for Health Award EP/Y020030/1. We acknowledge Rasha Abu-Eid for fruitful discussions.

References

- [1] Mikhail Binnewies, Edward W Roberts, Kelly Kersten, Vincent Chan, Douglas F Fearon, Miriam Merad, Lisa M Coussens, Dmitry I Gabrilovich, Suzanne Ostrand-Rosenberg, Catherine C Hedrick, et al. Understanding the tumor immune microenvironment (time) for effective therapy. *Nature medicine*, 24(5):541–550, 2018.
- [2] Wolf Herman Fridman, Franck Pagès, Catherine Sautès-Fridman, and Jérôme Galon. The immune contexture in human tumours: impact on clinical outcome. *Nature Reviews Cancer*, 12(4):298–306, 2012.
- [3] Valerie Chew, Han Chong Toh, and Jean-Pierre Abastado. Immune microenvironment in tumor progression: characteristics and challenges for therapy. *Journal of oncology*, 2012, 2012.
- [4] Simon Graham, Mostafa Jahanifar, Ayesha Azam, Mohammed Nimir, Yee-Wah Tsang, Katherine Dodd, Emily Hero, Harvir Sahota, Atisha Tank, Ksenija Benes, et al. Lizard: a large-scale dataset for colonic nuclear instance segmentation and classification. In *Proceedings of the IEEE/CVF international conference on computer vision*, pages 684–693, 2021.
- [5] Simon Graham, Quoc Dang Vu, Shan E Ahmed Raza, Ayesha Azam, Yee Wah Tsang, Jin Tae Kwak, and Nasir Rajpoot. Hover-net: Simultaneous segmentation and classification of nuclei in multi-tissue histology images. *Medical image analysis*, 58:101563, 2019.
- [6] Alexander Kirillov, Eric Mintun, Nikhila Ravi, Hanzi Mao, Chloe Rolland, Laura Gustafson, Tete Xiao, Spencer Whitehead, Alexander C. Berg, Wan-Yen Lo, Piotr Dollár, and Ross Girshick. Segment anything, 2023.
- [7] Jia-Ren Lin, Yu-An Chen, Daniel Campton, Jeremy Cooper, Shannon Coy, Clarence Yapp, Juliann B Tefft, Erin McCarty, Keith L Ligon, Scott J Rodig, et al. High-plex immunofluorescence imaging and traditional histology of the same tissue section for discovering image-based biomarkers. *Nature cancer*, 4(7):1036–1052, 2023.
- [8] Ruchika Verma, Neeraj Kumar, Abhijeet Patil, Nikhil Cherian Kurian, Swapnil Rane, Simon Graham, Quoc Dang Vu, Mieke Zwager, Shan E Ahmed Raza, Nasir Rajpoot, et al. Monusac2020: A multi-organ nuclei segmentation and classification challenge. *IEEE Transactions on Medical Imaging*, 40(12):3413–3423, 2021.
- [9] Jevgenij Gamper, Navid Alemi Koohbanani, Ksenija Benes, Simon Graham, Mostafa Jahanifar, Syed Ali Khurram, Ayesha Azam, Katherine Hewitt, and Nasir Rajpoot. Pannuke dataset extension, insights and baselines. *arXiv preprint arXiv:2003.10778*, 2020.
- [10] Mohamed Amgad, Lamees A Atteya, Hagar Hussein, Kareem Hosny Mohammed, Ehab Hafiz, Maha AT Elsebaie, Ahmed M Alhusseiny, Mohamed Atef AlMoslemany, Abdelmagid M Elmatboly, Philip A Pappalardo, et al. Nucls: A scalable crowdsourcing approach and dataset for nucleus classification and segmentation in breast cancer. *GigaScience*, 11:giac037, 2022.
- [11] Elaine L Alexander and Bruce Wetzel. Human lymphocytes: similarity of b and t cell surface morphology. *Science*, 188(4189):732–734, 1975.
- [12] Dmitry I Strokotov, Maxim A Yurkin, Konstantin V Gilev, Dirk R Van Bockstaele, Alfons G Hoekstra, Nikolay B Rubtsov, and Valeri P Maltsev. Is there a difference between t-and b-lymphocyte morphology? *Journal of biomedical optics*, 14(6):064036–064036, 2009.
- [13] Bernhard Mlecnik, Gabriela Bindea, Helen K Angell, Pauline Maby, Mihaela Angelova, David Tougeron, Sarah E Church, Lucie Lafontaine, Maria Fischer, Tessa Fredriksen, et al. Integrative analyses of colorectal cancer show immunoscore is a stronger predictor of patient survival than microsatellite instability. *Immunity*, 44(3):698–711, 2016.
- [14] Kai Wang, Tiansheng Shen, Gene P Siegal, and Shi Wei. The cd4/cd8 ratio of tumor-infiltrating lymphocytes at the tumor-host interface has prognostic value in triple-negative breast cancer. *Human pathology*, 69:110–117, 2017.